

## Ratchet Effect and the Transporting Islands in the Chaotic Sea

Lei Wang,<sup>1,2</sup> Giuliano Benenti,<sup>3,4</sup> Giulio Casati,<sup>3,4,1</sup> and Baowen Li<sup>1,5</sup>

<sup>1</sup>*Department of Physics and Centre for Computational Science and Engineering, National University of Singapore, Singapore 117542, Republic of Singapore*

<sup>2</sup>*Department of Physics, Renmin University of China, Beijing 100872, People's Republic of China*

<sup>3</sup>*CNISM, CNR-INFN, and Center for Nonlinear and Complex Systems, Università degli Studi dell'Insubria, Via Valleggio 11, 22100 Como, Italy*

<sup>4</sup>*Istituto Nazionale di Fisica Nucleare, Sezione di Milano, Via Celoria 16, 20133 Milano, Italy*

<sup>5</sup>*NUS Graduate School of Integrative Sciences and Engineering, Singapore 117597, Republic of Singapore*  
(Received 20 June 2007; published 14 December 2007)

We study directed transport in a classical deterministic dissipative system. We consider the generic case of mixed phase space and show that large ratchet currents can be generated thanks to the presence, in the Hamiltonian limit, of transporting stability islands embedded in the chaotic sea. Because of the simultaneous presence of chaos and dissipation the stationary value of the current is independent of initial conditions, except for initial states with very small measure.

DOI: [10.1103/PhysRevLett.99.244101](https://doi.org/10.1103/PhysRevLett.99.244101)

PACS numbers: 05.45.Pq, 05.60.Cd

The ratchet effect, that is, the possibility of obtaining directed transport of particles in the absence of any net bias force, is a problem at the heart of statistical mechanics. Ratchet transport in systems at equilibrium is forbidden by the second principle of thermodynamics [1]. On the other hand, it is possible to overcome this limitation in systems out of equilibrium, provided all space-time symmetries which inhibit directed motion are broken [2]. The ratchet phenomenon has recently gained renewed interest [3,4] as a model elucidating the physics of molecular motors [5]. Moreover, directed transport may lead to technological applications at the nanoscale [6], including new electron pumps, molecular switches, rectifiers, and transistors.

Previous theoretical studies have shown the ratchet effect in systems in which noise is absent and its role is played by the deterministic chaos induced by the inertial term [7]. In particular, the origin of current reversal in such inertia ratchets has been carefully investigated [8].

In spite of these pioneering works, the interrelation between the complexity and the rich variety of classical chaotic motion in conservative systems and the appearance of the ratchet phenomenon when dissipation is introduced is not known. In particular, the role of stable islands in the mixed phase space structure which is *generic* in nonlinear dynamical systems is not clear [9].

In this Letter, by considering a periodically kicked, dissipative, inertia ratchet, we show that the generic mixed phase space structure of the conservative case may lead to a strong ratchet phenomenon when dissipation is introduced. In particular, for strong dissipation, large currents may arise in a short time scale. On the other hand, for weak dissipation, large ratchet currents can be achieved nearly independently of initial conditions, as a result of a beautiful interplay between chaotic diffusion, ballistic transport of islands, and dissipation.

The system we study is a particle moving in one dimension  $[x \in (-\infty, \infty)]$  in a periodic kicked asymmetric potential:

$$V(x, \tau) = K \left[ \cos(x) + \frac{a}{2} \cos(2x + \phi) \right] \sum_{m=-\infty}^{\infty} \delta(\tau - mT), \quad (1)$$

where  $T$  is the kicking period, which is set to unity in this Letter. The evolution of the system in one period is described by the map

$$\begin{cases} \bar{p} = \gamma p + K[\sin(x) + a \sin(2x + \phi)], \\ \bar{x} = x + \bar{p}, \end{cases} \quad (2)$$

where  $p$  is the momentum variable conjugated to  $x$  and  $\gamma \in [0, 1]$  is the dissipation parameter, describing a velocity proportional damping. The limiting cases  $\gamma = 0$  and  $\gamma = 1$  correspond to overdamping and Hamiltonian evo-

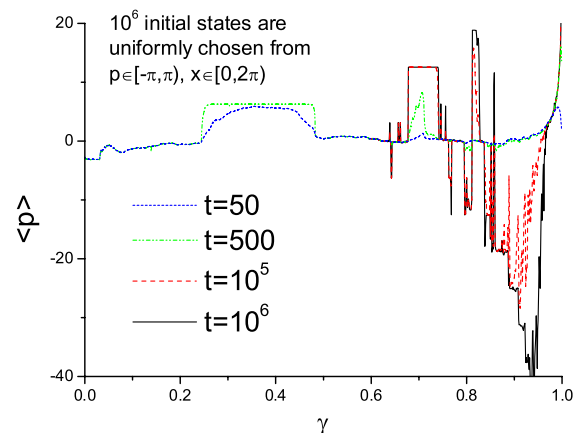


FIG. 1 (color online). Ensemble average current  $\langle p \rangle$  at different times, for  $a = 0.5$ .

lution, respectively. The spatial symmetry is broken at  $a \neq 0$ ,  $\phi \neq n\pi$ , with  $n$  integer [12]. However, directed transport is forbidden in the Hamiltonian limit due to time-reversal symmetry [13]. In this limit system (2) exhibits the typical mixed phase space structure. A central point of this Letter is to show that even very tiny, almost invisible islands, embedded in the chaotic sea play a crucial role in the generation of large ratchet currents when a small dissipation is added.

In Fig. 1 we plot the ratchet current  $\langle p \rangle$  as a function of the dissipation parameter  $\gamma$  at different times  $t$  (the discrete time  $t$  measures the number of kicks). Here we set  $K = 6.5$ ,  $a = 0.5$ ,  $\phi = \pi/2$ , and we follow the evolution in time of a large number of trajectories whose initial conditions are randomly and uniformly distributed in the *unit cell*  $-\pi \leq p < \pi$ ,  $0 \leq x < 2\pi$ . Therefore, the initial average momentum is  $\langle p \rangle = 0$  for any  $\gamma$ . Since all relevant space-time symmetries [2] are broken at  $\gamma \neq 1$ , then a directed current  $\langle p \rangle \neq 0$  can be generated. The dependence of the current on  $\gamma$  is rather complicated. In particular, we can see plateau regions inside which the asymptotic ratchet current is independent of  $\gamma$ . We note that for strong dissipation ( $\gamma \leq 0.6$ ) the current converges to its asymptotic value very rapidly and typically independently of initial conditions, the dynamics being characterized by a single stationary distribution. The weakly dissipative regime will be discussed later.

In order to understand the behavior of the ratchet current we first perform a linear stability analysis of map (2). The fixed points of the map when  $x$  is taken modulo  $2\pi$  are given by

$$\begin{cases} p^* = 2l\pi, l \text{ integer,} \\ (\gamma - 1)2l\pi + K[\sin(x^*) + a \cos(2x^*)] = 0, \end{cases} \quad (3)$$

where for the sake of simplicity we have considered the case  $\phi = \pi/2$ . The stability of these fixed points is determined by the eigenvalues  $\lambda_{1,2}$  of the Jacobian

$$\frac{\partial(\bar{p}, \bar{x})}{\partial(p, x)} = \begin{pmatrix} \gamma & K[\cos(x) - 2a \sin(2x)] \\ \gamma & 1 + K[\cos(x) - 2a \sin(2x)] \end{pmatrix}. \quad (4)$$

The modules  $|\lambda_{1,2}|$  versus  $x$  are shown in Fig. 2(a) for different  $\gamma$ . The stable intervals, in which the modules of the eigenvalues are both less than 1, depend only very slightly on  $\gamma$ . Therefore we may consider the case  $\gamma = 1$ , for which the stability intervals can be computed analytically and are given by  $(\arcsin\frac{1}{4a}, \frac{\pi}{2})$ ,  $(\pi - \arcsin\frac{1}{4a}, c_1)$ ,  $(c_2, \frac{3\pi}{2})$ , where  $c_1, c_2$  are the real roots of the equation  $\cos(x) - 2a \sin(2x) = -\frac{4}{K}$ . These intervals are shown as shadowed regions in Fig. 2(b).

As illustrated in Fig. 2(b), the fixed points  $(x^*, p^* = 2\pi l)$  can be determined graphically. If  $x^*$  resides in a shadowed region, then the fixed point is stable. Clearly there are no stable fixed points for  $l = 0$ . Instead, for any positive integer  $l$ , stable fixed points exist from  $\gamma = 1 -$

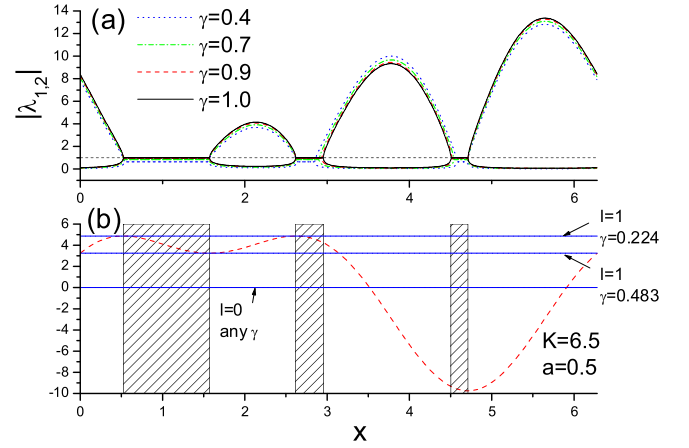


FIG. 2 (color online). (a) Modules of the eigenvalues  $\lambda_{1,2}(x)$  of the stability matrix (4) for different values of  $\gamma$ . (b) Dashed curve:  $f(x) = K[\sin(x) + a \cos(2x)]$ ; solid lines:  $g(x) = (1 - \gamma)2l\pi$  for different  $l$  and  $\gamma$ . In the shadowed regions,  $|\lambda_{1,2}(x)|$  are both less than 1.

$$\frac{K(a + \frac{1}{8a})}{2\pi l} = 1 - \frac{0.77588\dots}{l} \quad \text{to} \quad \gamma = 1 - \frac{K(1-a)}{2\pi l} = 1 - \frac{0.51725\dots}{l} \quad [14].$$

The bifurcation diagram of Fig. 3 confirms the above analytical estimates. The positions of the main fixed point windows ( $l = 1, 2, 3$ ) coincide with the plateaus  $\langle p \rangle = 2\pi, 4\pi, 6\pi$  observed in Fig. 1. At both ends of the fixed point windows tangent bifurcations occur which correspond to transitions from simple to strange attractors. (A similar picture holds for stable periodic orbits, even though their positions cannot be so easily calculated analytically.)

Since the width of the  $l$ th stability window is proportional to  $\frac{1}{l}$  and  $\sum_{l=1}^{\infty} \frac{1}{l}$  does not converge, these windows

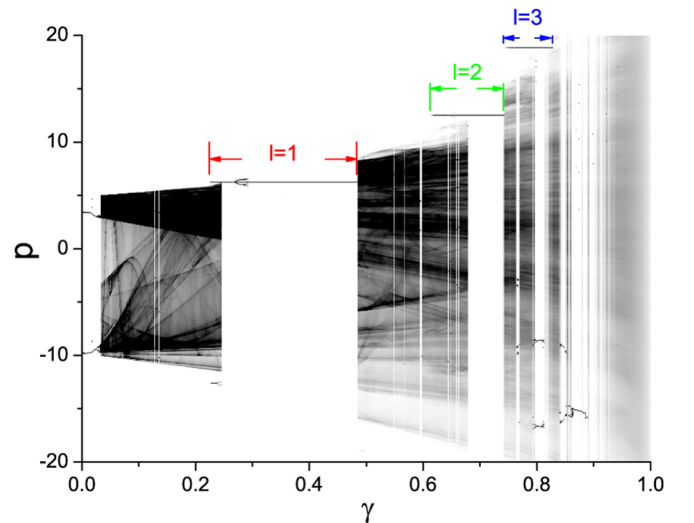


FIG. 3 (color online). Bifurcation diagram:  $5 \times 10^3$  iterates are drawn after a transient of  $10^5$  map steps, starting from 3600 initial states drawn from a uniform distribution in the unit cell  $0 \leq x < 2\pi$ ,  $-\pi \leq p < \pi$ . The analytical expectations for the position of fixed point windows at  $a = 0.5$  are also indicated.

must overlap when  $l$  is large enough. Therefore, multiple attractors (and also periodic orbits) must coexist when  $\gamma$  approaches 1. Their attractive basins cut the phase space into many pieces and here one may expect the asymptotic ratchet current to depend, in general, on initial conditions. The large negative values of  $\langle p \rangle$  that appear at long times in Fig. 1 are the consequence of trajectories ending up on periodic orbits after a long transient chaotic motion.

For very small dissipation ( $\gamma \gtrsim 0.98$ ), we could observe chaotic motion only on a fractal set even though it cannot be excluded that this is a transient with a lifetime much exceeding the total integration time. On the other hand, this weakly dissipative regime possesses very interesting features. Because of chaotic diffusion, the momentum probability distribution (Fig. 4) widens in time and eventually, due to dissipation, saturates to a stationary distribution close to a Gaussian. This is clearly seen in Fig. 4 in which the most remarkable feature is the small peak moving ballistically in the direction of positive  $p$ . This peak is due to the presence of small stability islands in the Hamiltonian limit  $\gamma = 1$  and plays a key role in the generation of the ratchet current.

To illustrate this point, we plot in Fig. 5 the evolution in time of the first two moments of the probability distribution  $P(p)$  and compare two different cases corresponding to two different initial conditions: (i) uniform distribution inside the unit cell  $p \in [-\pi, \pi]$ ,  $x \in [0, 2\pi)$  and (ii) uniform distribution inside the main transporting stability island. This island, for  $\gamma = 1$ , corresponds to ballistic motion in the positive momentum direction (“accelerator mode”), with the momentum increased of  $4\pi$  every 3 map iterations. Indeed this island is centered around the periodic orbit  $(x_1, p_1) \approx (1.6073, 4.9802) \rightarrow (x_2, p_2) \approx (2.9103, 1.303) \rightarrow (x_3, p_3) \approx (2.9103, 0) \rightarrow (x_4, p_4) = (x_1, p_1 + 4\pi = p_1)$  (here  $x$  and  $p$  are taken modulo  $2\pi$ ). The area of the island  $\approx 10^{-3}$ , that is, only  $3 \times 10^{-5}$  of the

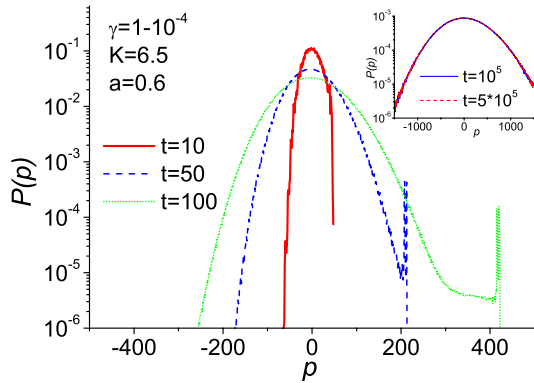


FIG. 4 (color online). Snapshots of the momentum probability distribution for  $1 - \gamma = 10^{-4}$ , starting from  $3.6 \times 10^9$  initial conditions randomly and uniformly chosen inside the unit cell  $p \in [-\pi, \pi]$ ,  $x \in [0, 2\pi)$ . In the inset the two curves drawn after long integration times,  $t = 10^5$  and  $t = 5 \times 10^5$ , overlap. This indicates that the distribution saturates (at least up to the integration times explored in our numerical simulations).

available phase space. Notwithstanding the accelerator mode, the ratchet current averages to zero in the Hamiltonian limit: a sum rule exists [10] such that the motion of the islands in the direction of positive momentum is balanced by the motion of the chaotic sea in the opposite direction. This sum rule no longer applies when dissipation is included since the latter mixes the sets which are invariant in the Hamiltonian limit, namely, the islands and the chaotic sea. Still, if dissipation is weak, these two sets remain essentially disconnected for a long time scale  $t_m \propto \frac{1}{1-\gamma}$ . As a consequence, as shown in Fig. 5, for  $t < t_m$  the ratchet current  $\langle p \rangle \approx 0$  when starting from the entire unit cell, while it grows linearly in time when the initial distribution is concentrated inside the island. In this latter case, as expected, the acceleration of the island is  $\frac{2}{3}(2\pi)$ ; that is, the island is shifted along  $p$  by 2 unit cells every 3 map iterations. At  $t \sim t_m$ , a momentum high enough is reached to allow dissipation to drive particles outside the island. Then the motion of these particles becomes chaotic and therefore the second moment of the distribution suddenly increases, while the first moment decreases due to dissipation. Correspondingly, for the initial condition inside the entire unit cell, the ratchet current starts to increase at  $t \sim t_m$  until the asymptotic value is reached [15]. This provides direct numerical evidence that the ratchet current is generated due to the presence of integrable islands in the Hamiltonian limit, the island and the chaotic sea being finally mixed by dissipation.

We would like to stress that, thanks to the presence of integrable islands in the Hamiltonian limit, large ratchet

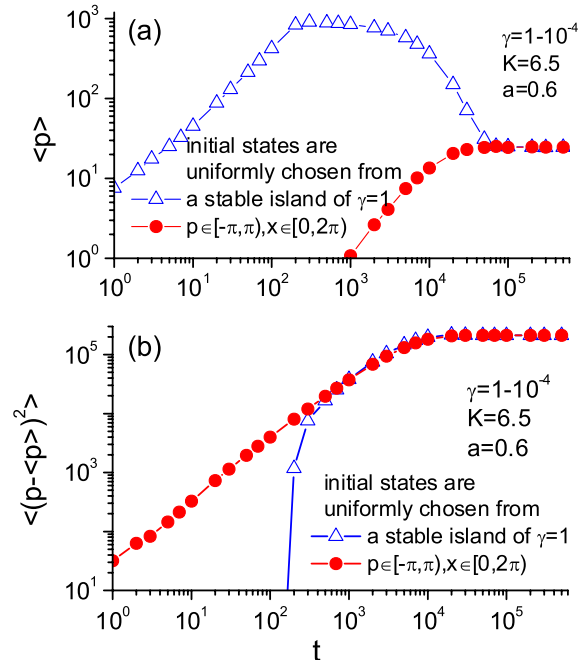


FIG. 5 (color online). First and second moment of the distribution  $P(p)$  as a function of time, for two different initial distributions.

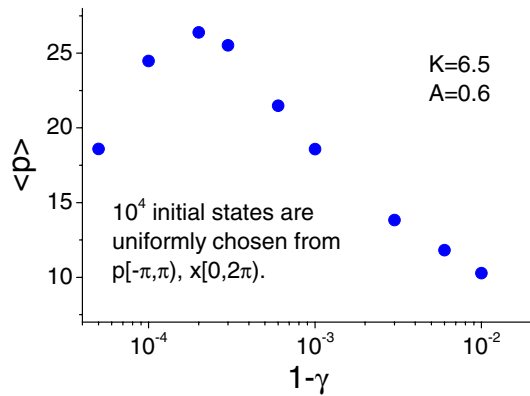


FIG. 6 (color online). Stationary ratchet current in the weak dissipation regime. The current is averaged over  $2 \times 10^7$  map iterations, taken after an initial transient of  $2 \times 10^7$  map steps.

currents can be achieved also for weak dissipation: as shown in Fig. 6, we can have  $\langle p \rangle > 26$ .

A completely different behavior takes place when this structure of islands is absent. Consider, for example, the ratchet model:

$$\begin{cases} \bar{p} = \gamma p + K[x - \pi - a \cos(x)], \\ \bar{x} = x + \bar{p}. \end{cases} \quad (5)$$

This map, in the Hamiltonian limit and for  $a \in [0, 1)$ , is completely chaotic with no stability islands [16]. For this map, we have always found as stationary distribution a strange attractor, supporting a very weak ratchet current. For instance, at  $K = 1$ ,  $a = 0.7$  we have obtained  $\langle p \rangle < 0.13$  for any value of  $\gamma$ . Basically the ratchet current is due only to the asymmetry of the attracting set which, at least for weak dissipation, is also weak.

In summary, the results presented in this Letter show that large ratchet currents can be generated in a dissipative system thanks to the presence, in the Hamiltonian limit, of transporting integrable islands embedded in a chaotic sea. This phenomenon leads, due to the joint presence of chaos and dissipation, to large ratchet currents nearly independently of initial conditions and is generic for systems with spatial and temporal periodicity, in that transporting islands are typical for such systems in the Hamiltonian limit.

Finally, we point out that the dissipative ratchet model discussed in this Letter could be realized by means of cold atoms in optical lattices, where it is possible to implement the asymmetric potential (1) [17] and a velocity proportional damping [18]. Since kicked systems similar to ours have been implemented in the deep quantum regime [19], it appears possible to investigate experimentally the impact of purely quantum effects such as dynamical localization on the ratchet transport discussed in this Letter.

We thank Gabriel Carlo for useful discussions. This work is supported in part by an Academic Research Grant from MOE.

- [1] R.P. Feynman, R.B. Leighton, and M. Sands, *The Feynman Lectures on Physics* (Addison-Wesley, Reading, MA, 1966), Vol. 1, Chap. 46.
- [2] S. Flach, O. Yevtushenko, and Y. Zolotaryuk, Phys. Rev. Lett. **84**, 2358 (2000); I. Goychuk and P. Hänggi, J. Phys. Chem. B **105**, 6642 (2001).
- [3] R.D. Astumian and P. Hänggi, Phys. Today **55**, No. 11, 33 (2002).
- [4] P. Reimann and P. Hänggi, Appl. Phys. A **75**, 169 (2002).
- [5] F. Jülicher, A. Ajdari, and J. Prost, Rev. Mod. Phys. **69**, 1269 (1997).
- [6] Special issue on *Ratchets and Brownian Motors: Basics, Experiments and Applications*, edited by H. Linke [Appl. Phys. A **75**, 167 (2002)].
- [7] P. Jung, J.G. Kissner, and P. Hänggi, Phys. Rev. Lett. **76**, 3436 (1996).
- [8] J.L. Mateos, Phys. Rev. Lett. **84**, 258 (2000).
- [9] Note, however, that, in the Hamiltonian limit, the ratchet effect in systems with mixed phase space dynamics is discussed in [2,10,11].
- [10] H. Schanz, M.-F. Otto, R. Ketzmerick, and T. Dittrich, Phys. Rev. Lett. **87**, 070601 (2001).
- [11] J. Gong and P. Brumer, Phys. Rev. E **70**, 016202 (2004); A. Kenfack, S.M. Sweetnam, and A.K. Pattanayak, Phys. Rev. E **75**, 056215 (2007).
- [12] Note that at  $a = 0$  map (2) reduces to the Zaslavsky map, a paradigmatic model in the study of dissipative chaotic systems; see R.Z. Sagdeev, D.A. Usikov, and G.M. Zaslavsky, *Nonlinear Physics* (Harwood Academic Publishers, New York, 1988). In this limit the potential  $V(x, t)$  becomes symmetric (for  $x \rightarrow -x$ ), and therefore the ratchet effect is absent.
- [13] We note that the quantum version of map (2) for a particular set of parameters has been recently studied in G.G. Carlo, G. Benenti, G. Casati, and D.L. Shepelyansky, Phys. Rev. Lett. **94**, 164101 (2005); see also Ref. [2].
- [14] Note that there also exist stable fixed points for negative integers  $l$  when  $l \leq -2$ ; however, we have observed in our numerical simulations that their effect on the ratchet current is very small.
- [15] Note that in this case the growth of variance  $\sigma_p^2(t) = \langle (p(t) - \langle p(t) \rangle)^2 \rangle$  of the momentum fluctuations in  $p(t)$  [circles in Fig. 5(b)] is closely described by an effective, diffusive Ornstein-Uhlenbeck process  $u(t)$  with drift  $-(1 - \gamma)u(t)$  and diffusion constant  $D \propto K^2$ , so that  $\sigma_p^2(t) \approx \frac{D(1 - e^{-2(1-\gamma)t})}{1-\gamma}$ , which turns out to be in very good agreement with our numerical data.
- [16] C. Liverani and M. Martens, Commun. Math. Phys. **260**, 527 (2005).
- [17] G. Ritt, C. Geckeler, T. Salger, G. Cennini, and M. Weitz, Phys. Rev. A **74**, 063622 (2006).
- [18] M.O. Scully and M.S. Zubairy, *Quantum Optics* (Cambridge University Press, Cambridge, England, 1997).
- [19] M.G. Raizen, V. Milner, W.H. Oskay, and D.A. Steck, in *New Directions in Quantum Chaos*, Proceedings of the ‘‘E. Fermi’’ Varenna School, edited by G. Casati, I. Guarneri, and U. Smilansky (IOS Press, Amsterdam, 2000).